SPACE TELESCOPE SCIENCE INSTITUTE
Operated for NASA by AURA

Instrument Science Report WFC 2013-01

WFC3/IR Spatial Sensitivity Test

Tomas Dahlen

January 4, 2013

Abstract

Here we present details on the WFC3/IR spatial sensitivity test. The aim of the test is to observe a standard star in a grid pattern covering the IR detector to investigate spatial variations in the measured photometry. Any deviations from a uniform response could be due to errors in the flat field calibration file. We find that the current pipe-line IR flat-fields, which are a combination of a ground-based high frequency (pixel-to-pixel) component and a low frequency correction based on in-flight sky observations, produces stable photometry over most of the detector. We estimate that the typical rms in measured photometry due to the flat field uncertainties is less than ∼0.007 mag. We do not find any significant low frequency large scale gradients in the photometry, except possibly for a region near the bottom left of the detector. Overall, these test indicates that the IR flat fields produce consistent photometry over the central 800x800 pixels of the detector investigated here.

1. Introduction

During data calibration, the flat fielding process corrects for pixel-to-pixel variations in the detector response and for imperfections in the optical path, such as dust grains on filters or other optical surfaces. Ideally, after flat fielding the photometry of a particular source should remain constant (within photometric errors) regardless of where on the detector it falls. To achieve this, accurate flat field calibration files are required. The initial flat field files used to calibrate data acquired after the installation of the Wide Field Camera 3 (WFC3) on board the *Hubble Space Telescope* during Servicing Mission 4 in May 2009, were created on the ground during the Thermal Vacuum 3 (TV3) testing in the spring

of 2008. These flat fields were obtained using an external optical stimulus (CASTLE) as the illumination source (Bushouse 2008). In order to investigate the quality of these initial WFC3 flat fields, calibration programs were carried out during both Servicing Mission Observatory Verification 4 (SMOV4, proposal CAL-11453) and subsequent normal calibration cycles (proposals CAL-11928 during Cycle 17 and CAL-12340 during Cycle 18). As a test of the flat field calibration files, observations of star clusters 47 Tuc and Omega Cen taken at multiple dither positions and rotations angles were used to derive a map of low-frequency residuals in photometry as a function of position in the detector. The analysis performed for these programs were based on the same software and methodology as applied for the ACS low frequency flat corrections described in Mack et al. (2002) and van der Marel (2003). Tests using the F110W and F160W filters showed that the residuals had an rms of ∼1.1% and a peak-to-peak variation of ±2.5% in both filters. These residual low frequency structures are likely caused by differences in the ground-based (CASTLE) and in-flight optical paths. The results found suggested that updating the flat field calibration files could significantly improve the IR photometry.

The method adopted to derive new flat field calibration files is described in detail in Pirzkal et al. (2011). In short, thousands of IR observations that were already calibrated using the original ground based flat fields were combined to make a smoothed sky delta flat field. This flat field accounts for the differences in low frequency response due to the difference in ground-based and in-flight illumination. The initial comparisons of the structure of the delta sky flat field between filters and time epochs suggested that the corrections were both wavelength and time independent. Therefore, a single "gray" delta sky flat field correction was used to make low frequency corrections to all the ground-based TV3 flat fields. These new flat fields were ingested into CDBS on December 7th, 2010. Performed tests suggested that the photometric accuracy using these new flats should be better than 0.5%, with peak to peak variation of -1.5%/+1.6%, for a large part of the detector. The aim of this report is to describe the tests performed to further evaluate the spatial stability of the WFC3/IR photometry derived using these flat fields.

2. Spatial Stability Calibration Program

The calibration program 12708 "WFC3/IR Spatial Sensitivity" (PI: A Rajan) was carried out in May and September of 2012 during *HST* Cycle 19 to check the spatial stability of WFC3/IR observations after applying the flat field solutions derived by combining the ground based pixel-to-pixel flats with the low frequency corrections derived from the delta sky flat field as described above. To check the photometry, we stepped the standard star WD-1057+719 across the detector using a 21 point grid, where at each grid point two observations, slightly offset by ∼40 pixels, were obtained, sampling a total of 42 points on the detector. The filters used in this investigation were F098M, F125W, and

F160W and the total number of orbits used was four. The layout of the observations is shown in Figure 1. In the center of the detector, we used a 3 by 3 grid with the 512x512 pixel subarray. The use of a subarray allowed for short exposure times (4.3s) and decreased readout time, resulting in a larger number of exposures compared to using the full detector size. Along the edges of the detectors, however, we used the full detector size, since there are no pre-defined subarrays covering this area. The exposure time for this area is therefore longer (8.8s). As will be discussed further below, these short exposure times turned out to be just barely of sufficient signal-to-noise for the proposed tests. For the final visit, observed at a later epoch compared to the first three orbits, we adjusted the sampling sequence to allow longer exposure times (22.9s) and therefore obtain higher signal-to-noise. With this layout of the observations, we are effectively investigating the low frequency stability over the central ∼800x800 pixels of the detector. When planning the observations, we made sure that the standard star did not fall on areas affected by IR blobs. The IR blobs are areas of about 10-20 pixels in diameter that show a reduction in detector response of up to a few percent (Pirzkal et al. 2010; Pirzkal & Hilbert 2012). In total, the IR blobs affect $\sim 1\%$ of the detector area. Figure 1 illustrates the locations of the different exposure times as well as the positions of the IR blobs.

3. Results

The data were reduced using the standard pipeline calibration software *calwf3*. Photometry was performed running the IRAF task *phot* on the calibrated flt.fits files after these were multiplied by the pixel area map, which corrects photometry for geometric distortion. We obtained aperture photometry with a radius of 10 pixels. To quantify the photometric stability over the detector, we calculate the mean flux of all positions and then derive the flux relative to this mean at each position. In Figure 2, we show the relative photometry at the 42 different positions in the three filters used in the investigation. The figure shows results for filter F098M at top left, F125W at top right, and F160W at bottom left, respectively. The figure shows that the typical deviations are mostly small, a majority of points deviates less than 1%, but that there are also cases with deviations of a few per cent. We note here that the same "gray" low frequency flat field correction has been applied to all filters. Therefore, if there are any significant spatial biases in this correction, one would expect the offsets to be biased in a similar direction in all filters. As an example, looking at the top left corner shows that two filters have overestimated flux (F098M and F125W) while one filter has underestimated flux (F160W). These deviations should therefore not be introduced by the flat field correction, but could instead be due to either statistical uncertainties in the measured fluxes, or unaccounted for color dependent terms in the flat field. There are also cases where all three filters indicate deviations from unity in the same direction (e.g., top right corner and bottom left corner). This could be

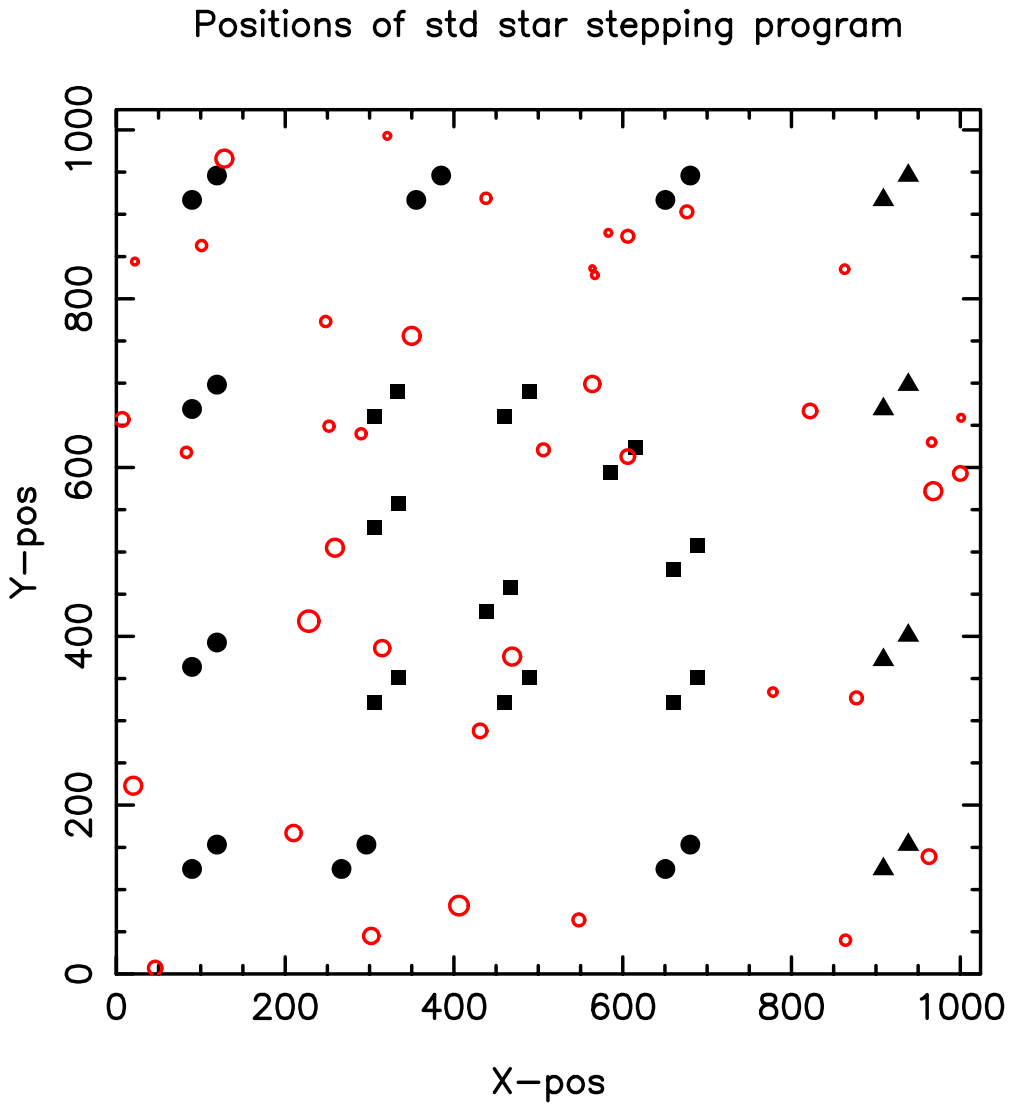

Fig. 1.— Black symbols show the positions of the standard star positions on the WFC3/IR detector. Different shapes indicate different exposure times (squares=4.3s, circles=8.8s, and triangles=22.9s). Red open circles indicate the positions and sizes of the IR blobs. We estimate that none of the measured standard star positions has photometry affected by the IR blobs.

due to the delta sky flat field, but may also be affected by statistical errors as we further examine below.

To quantify the deviations illustrated in Figure 2, we list the scatter around the mean in Table 1. The rms is shown for each filter including all 42 measurements, as well as divided into positions with different exposure times. The rms is given in magnitudes and has a

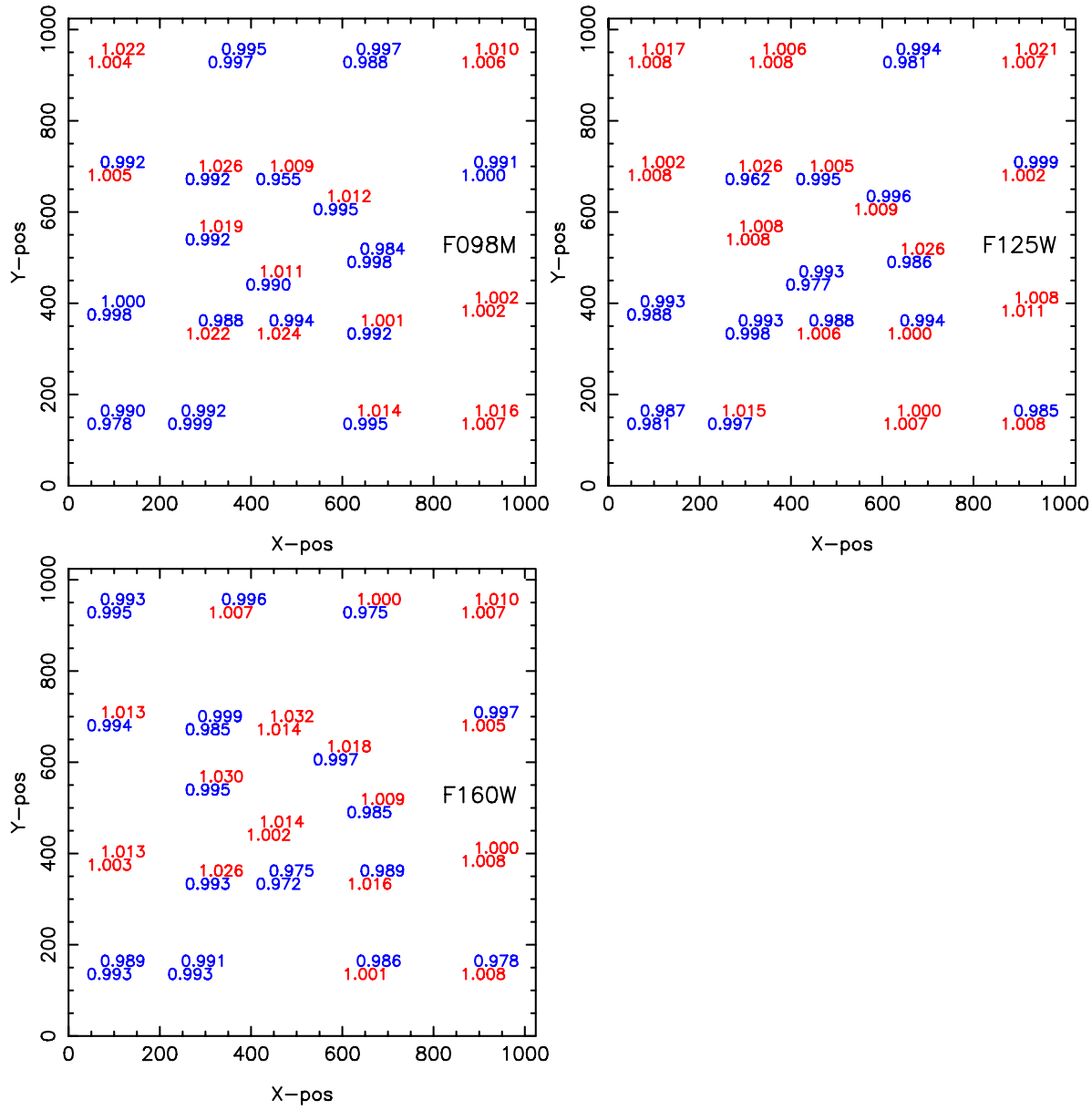

Fig. 2.— The flux as a function of position on the WFC3 IR detector derived from measurement of the standard star WD-1057+719 in three different filters, F098M (top left), F125W (top right), and F160W (bottom left). The flux is normalized by the mean flux in each filter, respectively. Values larger than one, in red, indicate that the measured photometry is brighter than the mean, while blue number indicates that the measured photometry is below the mean.

typical value of 0.014-0.015 mag. When looking at the scatter as a function of exposure

time, it is clear that the shorter exposure times have larger scatter, which should be due to lower signal-to-noise and therefore larger photometric errors for these observations. Looking at the photometric errors derived by the IRAF task *phot*, we find typical errors of 0.007-0.013 mag for the short 4.3s exposures, 0.004-0.007 mag for the intermediate 8.8s exposures, and 0.002-0.003 mag for the long 22.9s exposures. The photometric errors for short exposures are of the same order of magnitude as the measured scatter between measurements and could therefore contribute significantly to the latter. It is therefore likely that at least a fraction of the measured scatter is not due to the flat field, but instead due to insufficient signal-to-noise in the photometry.

Since any low frequency structure possibly introduced by the "gray" flat field correction should affect all filters in a similar way, we can add the results from the different filters to decrease statistical errors. The bottom line in Table 1 shows that the rms decreases significantly after combining results from the three filters. In fact, combining the results decreases the scatter by almost a factor sqrt(3), suggesting that a significant fraction of the measured scatter is indeed due to statistical photometric scatter and not caused by the flat field.

If there exists residual low frequency structures that are unaccounted for by the new flat field, it is expected that nearby positions on the detector would be biased in the same direction (as long as the scale corresponding to the low frequency structure is longer than the separation between points). Since at each position in the 21 point observing grid there are two measurements taken only ∼40 pixels (∼5 arcsec) apart, we can use the measured photometry to check for residual low frequency structures starting at these small scales. Inspecting the left panel of Figure 3 shows that about half of the positions have one overestimated and one underestimated measurement (one red and one blue), which is consistent with statistical fluctuations in the measured photometry or high frequency pixel-to-pixel uncertainties in the flat field. The only two positions that may be biased by low frequency structures (i.e., all are blue or all are red in the three filters) are the bottom left corner and the top right corner, where the former is the only position that consistently show a deviation of at least 1% in all measurements.

If we assume that there are no uncorrected structures in the flat fields at scales less than ∼40 pixels, we can average the photometry in each of the 21 measurement pairs to investigate biases at larger scales. In the right panel of Figure 3, we show the deviations in photometry at the 21 grid positions compared to the mean photometry. The overall rms is 0.006 mag with a peak to peak of -0.011/+0.015 mag. As noted before, it is mainly at the edge of the detector (bottom left corner) that we see a significant deviation (0.015 mag) suggesting that the flat fields does not properly correct this corner. Except at this position, we do not detect any significant gradients in the measured photometry, suggesting that the flat fielding works well. To further quantify this, we find when using only the nine central postions in the right panel of Figure 3 a peak to peak of -0.008/+0.009 mag and an rms of

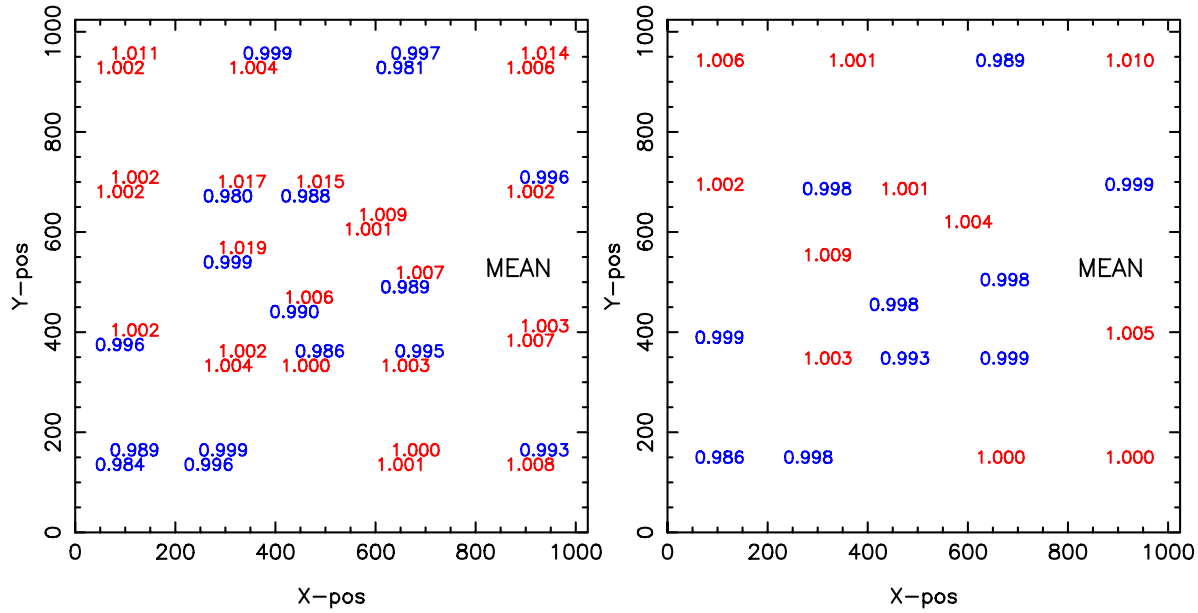

Fig. 3.— Left panel: Relative flux as a function of position on the WFC3 IR detector derived from measurement of the standard star WD-1057+719 after combining the results from the three filters F098M, F125W, and F160W. Flux values are first normalized by the mean in each separate filter and thereafter averaged. Values larger than one, in red, indicate that the measured photometry is brighter than the mean, while blue number indicates that the measured photometry is below the mean. Right panel: Relative flux as a function of position on the WFC3 IR detector after taking the mean flux in the nearby (∼40 pixel) position pairs in each filter and thereafter averaging over the three filters.

0.004 mag.

4. Summary and Conclusions

We have used the flux of the standard star WD-1057+719 measured at 42 different positions in three filters (F098M, F125W, and F160W) to investigate the spatial uniformity of the WFC3/IR photometry. The observations were taken at two epochs in May and September 2012 during *HST* Cycle 19. While the overall measured rms in photometry is $\sim$ 0.015 mag, we attribute a large fraction of this to photometric errors. The actual photometric uncertainty due to the flat field is estimated to be less that 0.007 mag. Furthermore, there is no apparent spatial gradient in the photometry derived using the current flat fields. However, there may be systematic errors of up to 0.015 mag in the photometry at the very edges of the detector. The highest deviations are noted within 200 pixels from the top right and the bottom left corners of the detector. It is important

to note that we have avoided the IR blobs when conducting these tests. Effects on the photometry due to these blobs are discussed in Pirzkal et al. (2010) and Pirzkal & Hilbert (2012). Future upgrades to the IR flat fields include an extended investigation of the color dependence of the sky flat fields and an improved characterization of the IR blobs and their temporal variation.

Acknowledgments

Thanks to Janice Lee whose review improved this manuscript.

References

Bushouse, H. 2008, WFC3 Instrument Science Report, WFC3-ISR - 2008–28 (Baltimore:STScI)

Mack, J., Bohlin, R., Gilliland, R., van der Marel,R., Blakeslee, J., & de Marchi, G. 2002, ACS Instrument Science Report, ACS-ISR - 2002–08 (Baltimore:STScI)

van der Marel, R. 2003, ACS Instrument Science Report, ACS-ISR - 2003–10 (Baltimore:STScI)

Pirzkal, N., Viana, A., & Rajan, A. 2010, WFC3 Instrument Science Report, WFC3-ISR - 2010–06 (Baltimore:STScI)

Pirzkal, N., Mack, J., Dahlen, T., & Sabbi, E. 2011, WFC3 Instrument Science Report, WFC3-ISR - 2011–11 (Baltimore:STScI)

Pirzkal, N., & Hilbert, B. 2012, WFC3 Instrument Science Report, WFC3-ISR - 2012–15 (Baltimore:STScI)

Table 1. Scatter in Photometry

Filter	All exp (N=42)	exp=4.3s (N=18)	exp=8.8s (N=16)	exp=22.9s (N=8)
F098M	0.014	0.019	0.011	0.007
F125W	0.014	0.016	0.012	0.011
F160W	0.015	0.019	0.010	0.011
Mean	0.009	0.012	0.008	0.007

Note. — The rms scatter given in magnitudes are shown of all 42 measurements per filter, as well as for measurements with different exposure times according to: 18 measurements with 4.3s, 16 measurements with 8.8s, and 8 measurements with 22.9s exposure time. Also shown are the results after taking the mean of the three different filters. Note the decrease in scatter at increased exposure time, indicating that scatter is affected by the signal-to-noise level.